

Processing, Structure, and Properties of Mullite Fiber/Mullite Matrix Composites

K. K. Chawla, Z. R. Xu & J.-S. Ha

Department of Materials and Metallurgical Engineering, New Mexico Institute of Mining and Technology, Socorro, New Mexico 87801, USA

(Accepted 22 July 1995)

Abstract

Oxide fiber/oxide matrix composites form an important and very attractive subpart of ceramic matrix composites because of their inherent stability in oxidizing atmospheres at high temperature. In particular, mullite fiber/mullite matrix composites have the potential of high temperature usage in oxidizing atmospheres.

The interface in mullite fiber/mullite matrix was engineered by using thick BN (1 μm) or BN/SiC double coating on mullite fibers, such that deformation mechanisms conducive to toughness enhancement could be brought to play. Significant improvements in the room temperature mechanical properties of these mullite fiber/mullite matrix composites could be achieved by incorporation of these interfacial coatings and by using a colloidal processing route to make dense mullite matrix.

Introduction

Ceramic matrix composites (CMCs) capable of maintaining excellent strength and fracture toughness are required for high temperature structural applications. Many of these applications require exposure to an oxidizing environment, as such the thermodynamic stability and oxidation resistance of CMCs become important issues. Nonoxide fiber/nonoxide matrix composites generally show good low temperature strength, but oxidation resistance is a major limitation.^{1,2} Nonoxide fiber/oxide matrix composites or oxide fiber/nonoxide matrix composites do not have high oxidation resistance because the permeability constant for the diffusion of oxygen is high, resulting in rapid oxygen permeation through the oxide matrix.³ It would thus appear that in applications where stability in air at high temperature is a prime objective, oxide fiber/oxide matrix composites should be considered because they are inherently stable in air.

Some oxide/oxide matrix composite systems have been investigated.^{4–7} A strong fiber/matrix bond forms in the oxide matrix reinforced with uncoated oxide fibers, such as in the like/like systems, (e.g. mullite/mullite)^{4,5} or in the mixed systems, (e.g. $\text{Al}_2\text{O}_3/\text{SiO}_2$)⁶ where additional compound(s) could form at the interface, and the overall mechanical properties of those composites were not much improved. As a consequence, a barrier layer is generally introduced to prevent fiber/matrix interaction, and thus, prevent strong interfacial chemical bonding. Carbon barrier coating has been frequently used in oxide/oxide composites.⁸ In this work on mullite/mullite composites, we have used BN and BN/SiC duplex coatings as interphase materials. We recognize that both BN and SiC are nonoxides, but are more oxidation resistant than carbon. Ideally, one would like to incorporate an oxide coating, but in this preliminary work we wish to explore the basic idea of mullite/mullite composites. If we can produce such composites with a BN or BN/SiC interphase without surface cracks, then oxygen ingress will be inhibited. The use of a BN coating is desirable because of its ease of sliding along the basal planes.⁹

Objective

The objectives of this work were to use an interface engineering approach, involving fiber coating, microstructure characterization of the interface, mechanical test and fractography study, in mullite/mullite systems to weaken the interfacial bond in order to achieve oxide/oxide composites with high work of fracture and a noncatastrophic failure mode.

Materials and Experimental Procedure

Mullite fibers, Nextel 480 and Nextel 550, both of 3M Co., were used in mullite matrix composites.

Table 1. Properties of fibers, mullite matrix, and fiber coatings

Properties	Nextel 480	Nextel 550	Mullite matrix ($3\text{Al}_2\text{O}_3\text{-}2\text{SiO}_2$)	Boron nitride (<i>h</i> -BN)	Silicon carbide (β -SiC)
Composition	70wt% Al_2O_3 28wt% SiO_2 2wt% B_2O_3	73wt% Al_2O_3 27wt% SiO_2	—	—	—
Melting point ($^{\circ}\text{C}$)	1850	1850	1850	3000	2220
Density (g/cm^3)	3.03	3.03	3.17	2.27	3.21
Strength ⁺ (MPa)	1900 [#] (Tensile)	2000 [#] (Tensile)	128–185	80–110	255–465*
Young's Modulus (GPa)	220	193	181	60–80*	440–470*
Coefficient of thermal expansion ($10^{-6}/^{\circ}\text{C}$)	4–5	4–5	4–5	5	4.8
Diameter (μm)	8×12	8×12	—	—	—
Reference	10	11	12–14	15–17	12, 18

⁺: At room temperature.

[#]: 51 mm gauge length.

*: Data of CVD materials.

Nextel 480 is a polycrystalline mullite fiber, while the as-received Nextel 550 is not crystalline mullite but a mixture of α -alumina and amorphous silica with mullite composition, which can be transformed to mullite when heated above 1200°C . Fiber coating of BN on Nextel 480 was applied by at Synterials Co. (Herndon, VA) using a proprietary CVD technique, and the double coating of BN/SiC on Nextel 550 was applied by 3M Co. (St. Paul, MN) via a proprietary CVD technique. In the double coating, the outer layer was SiC.¹⁰ The nominal compositions and some properties of the materials used are summarized in Table 1.^{11–19}

Conventional mullite powders need temperatures above 1500°C for considerable densification because of the low interdiffusion rates of silicon

and aluminum ions in crystalline mullite.^{18,19} Such high processing temperatures could cause severe damage on the fibers.⁴ The composite fabricated from the commercial mullite powder with uncoated Nextel 480 fiber showed fiber deformation and extensive interaction between the fiber and matrix, see Fig. 1. Note that large matrix grains had grown into the fiber due to the high processing temperature and pressure required for densification of the commercial mullite powders. The mullite matrix used in this work was obtained via a powder synthesized in our laboratory by a diphasic gel route using a boehmite (AlOOH) powder (Dispal 11N7, Remet Chemical Corp., Chadwicks, NY) and an amorphous silica sol (SP-30, Remet Chemical Corp.) as precursors. The gel was prepared by dispersing the boehmite powder in distilled water to get a boehmite sol, which was then mixed with the silica sol to have the stoichiometric mullite composition (71.8 wt.% Al_2O_3 and 28.2 wt.% SiO_2), followed by gelling at room temperature. The gel obtained was dried at 70°C and ground into powder form. All the composites were fabricated by slurry impregnation method.²² Consolidation of composites was done by hot-pressing. The composites were fabricated by infiltrating uncoated and coated fibers, Nextel 480, with a slurry of the matrix powder prepared with isopropanol and an organic binder, and unidirectionally laying the infiltrated fibers on mylar tapes. After drying, the prepared tapes were cut, stacked, and heated at 700°C for 2 h in air to remove the binder and the hydroxyl in the boehmite. Consolidation of composites was done by hot-pressing at 1300°C and 35 MPa for 1 h in vacuum. A part of the hot-

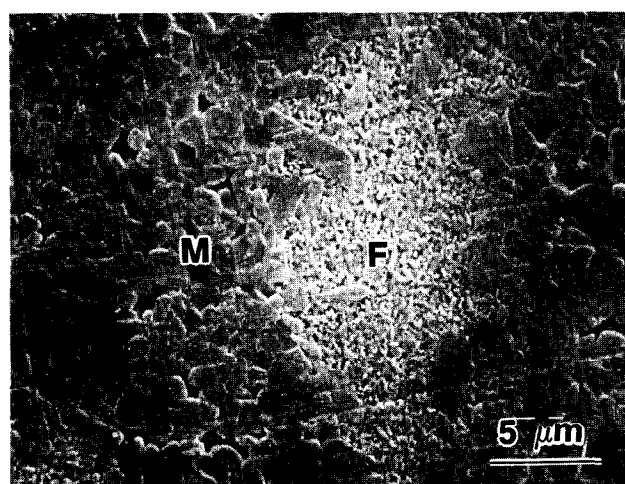


Fig. 1. Etched surface of uncoated Nextel 480/mullite composite fabricated with a commercial mullite powder as the matrix material. Note the extensive fiber (F)/matrix (M) interaction and fiber deformation.

pressed composite was cut and heat treated at 1320°C for 1 h in N₂, to cause produce complete crystallization of the mullite matrix, since it was found that the matrix in the as-hot-pressed composite did not crystallize. The details of processing have been reported elsewhere.^{23,24}

Optical and scanning electron microscopes were used for general characterization of the microstructure of the composites. Secondary ion mass spectrometry (SIMS) was used to identify the coatings in composites. Strength of composites was measured in three-point bend tests at room temperature using rectangular bar-shaped specimens with fiber direction parallel to the length of the specimen. Work of fracture (WOF) and the critical stress intensity factor of the composites were measured at room temperature using Chevron-notched bar specimen in three-point bend tests. The frictional shear stress in the BN coated Nextel 480/mullite composite was measured using an interfacial testing system (ITS). The details of this method have been published in Ref. 25.

Results and Discussion

Characterization of the interface

Figure 2(a) shows the cross-section of the BN coated Nextel 480 fiber, with coating thickness being about 1 μm . SIMS characterization verified that there was boron present, see Fig. 2(b). BN structure was turbostratic.²⁶ The microstructure of the BN/SiC coated Nextel 550 fiber, Fig. 3(a), shows that the fiber was fairly uniformly coated with two layers, BN and SiC, with thickness of about 0.1 and 0.2 μm , respectively. SIMS characterization also illustrated the presence of the double coating in the composites, Fig. 3(b and c). Such a thick (1 μm) BN coating was used to survive the processing conditions in order to provide a desired weak interface. By the same token, the outer SiC coating was used to protect the BN inner layer from oxidation during composite fabrication.

Typical raw load versus fiber-end displacement curves from single fiber pushout tests are shown in Fig. 4 (a and b). Note that after fiber pushout, which coincides with load drop, the curve rises with upward concavity. This is because the 10 μm flat-bottomed indenter is very close in dimension to the minor axis of the fiber and soon after fiber pushout the indenter starts loading the matrix. Figure 5 shows the stress versus fiber-end displacement curve after correcting for the contribution of the load train compliance to the total measured displacement. The load train compliance is determined from load versus displacement curves

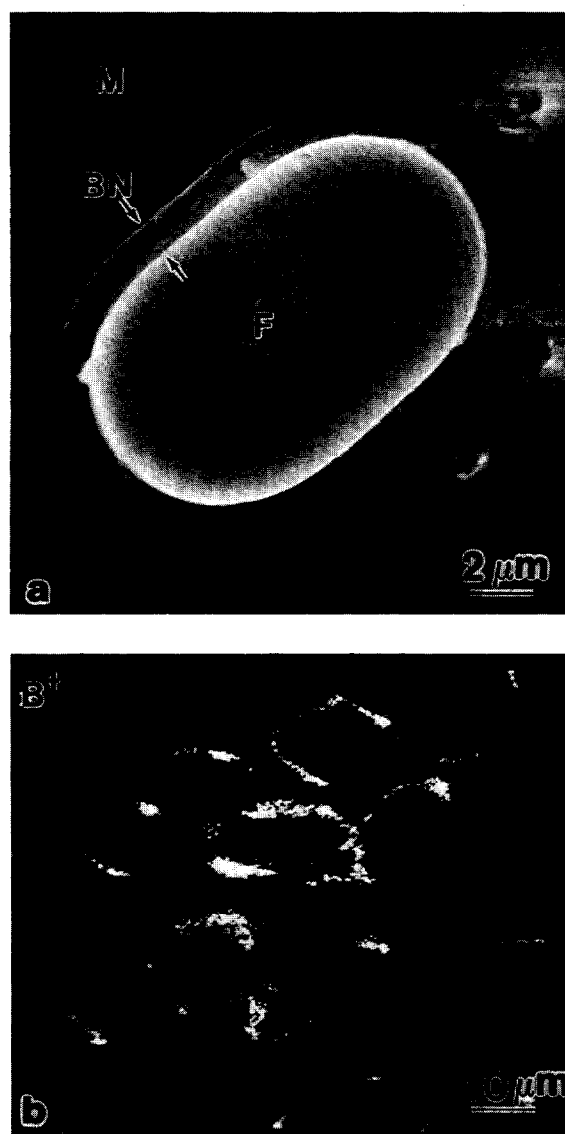


Fig. 2. (a) Cross-section of a BN-coated Nextel 480 fiber, showing the coating thickness 1 μm , (M: matrix, F: fiber); (b) B⁺ mapping by SIMS in a BN-coated Nextel 480/mullite composite.

obtained by subjecting the sample to compression at various points along the wedge by means of a 500 μm diameter stainless steel rod. Typical values for the compliance of the ITS system and wedged continuous fiber reinforced ceramic composite sample are between 4 and 6 $\mu\text{m}/\text{N}$.²⁷ Also shown is the best fit of the data (from the initiation of debonding to the point of fiber pushout) using the progressive fiber debonding and sliding model of Hsueh.²⁸ It should be pointed out that the predictions of the strength-based model of Hsueh are equivalent to those of the energy-based model of Kerans and Parthasarathy.^{27,29} The frictional shear stress in the present system was about 50 MPa.

Mechanical properties

The density, fiber volume fraction, and phases of the composites are listed in Table 2. It can be seen from this table that the matrix in the as-hot-



Fig. 3. (a) Cross-section of a SiC/BN coating Nextel 550 fiber, showing the double coating, (M: matrix, F: fiber); (b and c) SIMS analysis of the surface of a SiC/BN-coated Nextel 550/mullite composite, showing the presence of boron and silicon.

pressed composites did not transform to crystallize mullite at the hot pressing temperature. However, a complete mullite crystallization of the mullite matrix was achieved after the heat treatment (see the section on Materials and Experimental Procedure).

The bend strength, work of fracture, and criti-

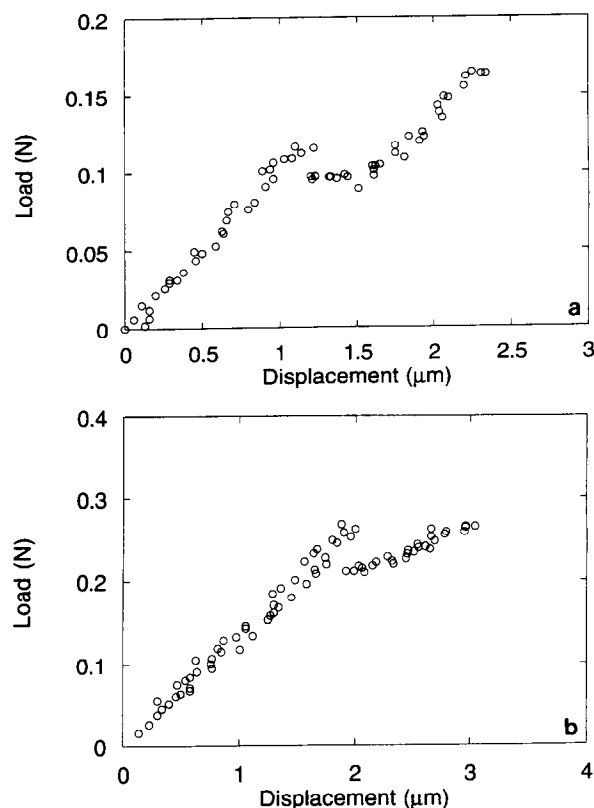


Fig. 4. (a and b) Typical raw load versus fiber-end displacement curves from single fiber pushout tests. Note that after the fiber pushout, which coincides with load drop, the curve rises with upward concavity. This is because soon after debonding the indenter starts loading the matrix.

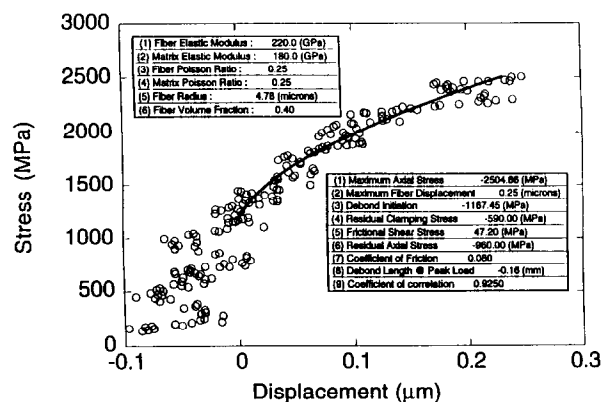


Fig. 5. Stress versus fiber-end displacement curve after correcting for the contribution of the load train compliance to the total measured displacement. Also shown is the best fit of the data (from the initiation of debonding to the point of fiber pushout) using the progressive fiber debonding and sliding model of Hsueh.²⁵

cal stress intensity factors for mullite/mullite composites are listed in Table 3. As can be seen, significant improvements, especially in fracture toughness, were obtained in the interface engineered mullite/mullite composites.

The composite with 1 μm BN coated Nextel 480 exhibited damage tolerant characteristics with a load-bearing capacity even beyond the maximum load, as indicated by a gradual load drop which continued up to a significant amount of displace-

Table 2. Density, fiber volume fraction, and phases of the composites

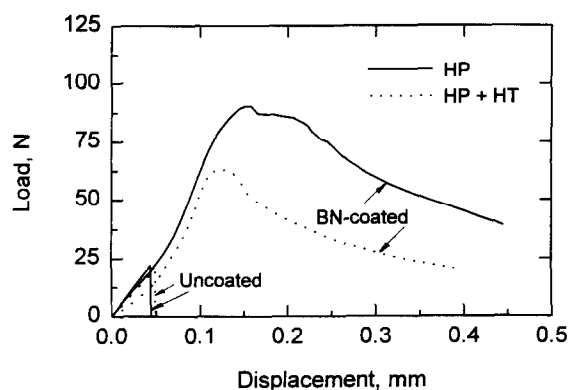
	Nextel 480/BN/mullite	Nextel 550/BN/SiC/mullite
Density(%) [#]	90	85
Fiber volume fraction, V_f	0.41	0.33
Phase		
As-HP [†]	$a + s + m^*$	$a + s^*$
HP+HT [‡]	Mullite	Mullite

[#]Relative densities to the theoretical composite densities calculated using a rule of mixture.

[†] As hot pressed.

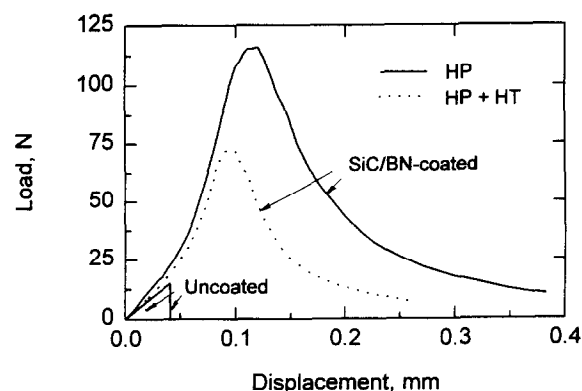
[‡] As hot pressed and heat treated.

* a , s and m denote δ -alumina, amorphous silica, and mullite, respectively.

**Fig. 6.** Load-displacement curves obtained in Chevron-notch tests for Nextel 480/BN/mullite composites in as hot-pressed and hot-pressed + heat-treated conditions.

ment without complete failure during the test, as seen in Fig. 6. After heat treatment leading to complete mullite crystallization of the matrix, this composite still showed a non-catastrophic failure, also shown in Fig. 6. The loss of fiber strength resulted from the heat treatment was responsible for the load drop to a certain level after heat treatment.

Similar to the composite with 1 μm BN coated Nextel 480 fibers, the composite with SiC/BN

**Fig. 7.** Load-displacement curves obtained in Chevron-notch tests for Nextel 550/BN/SiC/mullite composites in as hot-pressed and hot-pressed + heat-treated conditions.

double coated Nextel 550 fibers showed a non-brittle failure, see Fig. 7.

Scanning electron micrographs of the fracture surfaces obtained in three-point bend test of the mullite/mullite composites are shown in Figs 8, 9 and 10. The BN coating in Nextel 480/mullite was found on the pulled-out fiber surface with some peeling-off or separation from the fiber, see Fig. 8. This indicates that both the interfaces of matrix/coating and coating/fiber were weakly bonded. This is not surprising inasmuch as hexagonal BN shears easily. The pulled-out fiber surfaces in the BN/SiC coated Nextel 550/mullite composite were mostly clean and smooth, see Fig. 9. An SEM picture, Fig. 10, showing one of the holes formed in the matrix of Nextel 550/mullite composite as a result of the fiber pullout, reveals that the SiC and BN layers were intact in the matrix and a strong bonding was formed between the matrix and the SiC coating. This can be attributed to a relative strong bonding between SiC and matrix. Also, the BN thickness in double coating is very thin ($\sim 0.1 \mu\text{m}$). This indicates that, unlike Nextel 480/BN/mullite in which the fiber pullout could occur at

Table 3. Mechanical properties of the composites

Composite		V_f	$\sigma_{max}(\text{MPa})$	WOF (J/m^2)	$K_{IC} (\text{MPa m}^{1/2})$
Nextel 480/mullite:					
Uncoated	As-HP	0.45	104	56	1.8
	HP+HT	0.45	106	47	1.9
BN-coated	As-HP	0.41	322	2410	11.6
	AP+HT	0.41	258	1630	8.5
Nextel 550/mullite:					
Uncoated	As-HP	0.47	87	18	1.5
	HP+HT	0.47	71	12	1.4
BN-coated	As-HP	0.33	182	733	7.1
	HP + HT	0.33	223	308	6.0

As-HP: as hot pressed; HP+HT: as hot pressed and heat treated.

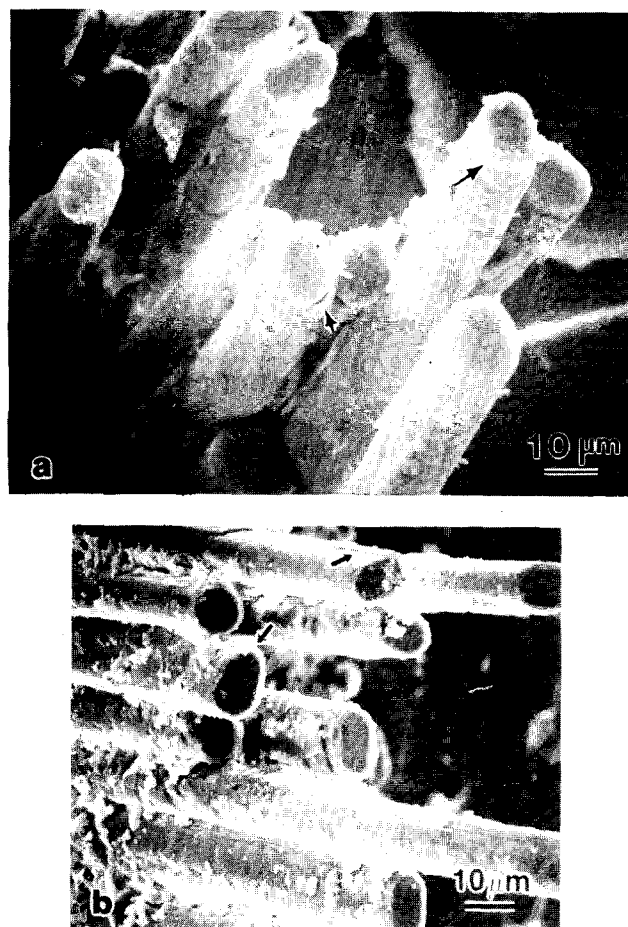


Fig. 8. Fracture surface of BN-coated Nextel 480/mullite composites: (a) hot-pressed and (b) hot-pressed + heat-treated, arrows showing the separation or peeling off of the BN coating.

the interfaces of either matrix/coating or coating/fiber, the fiber pullout occurred along the interface of the fiber and BN coating only.

Conclusions

The fiber/matrix interaction in mullite fiber/mullite matrix composites during processing can be effectively controlled by interface engineering approach. These engineered interfaces consisting of thick BN or a double BN/SiC coating coupled with the colloidal processing to consolidate the mullite matrix at a relatively low temperature, allowed us to make mullite fiber/mullite matrix composites showing high work of fracture and a noncatastrophic failure mode at room temperature.

Acknowledgements

This work was supported by the office of Naval Research, Contract No. N0014-89-J1459 and was monitored by Dr S. G. Fishman.

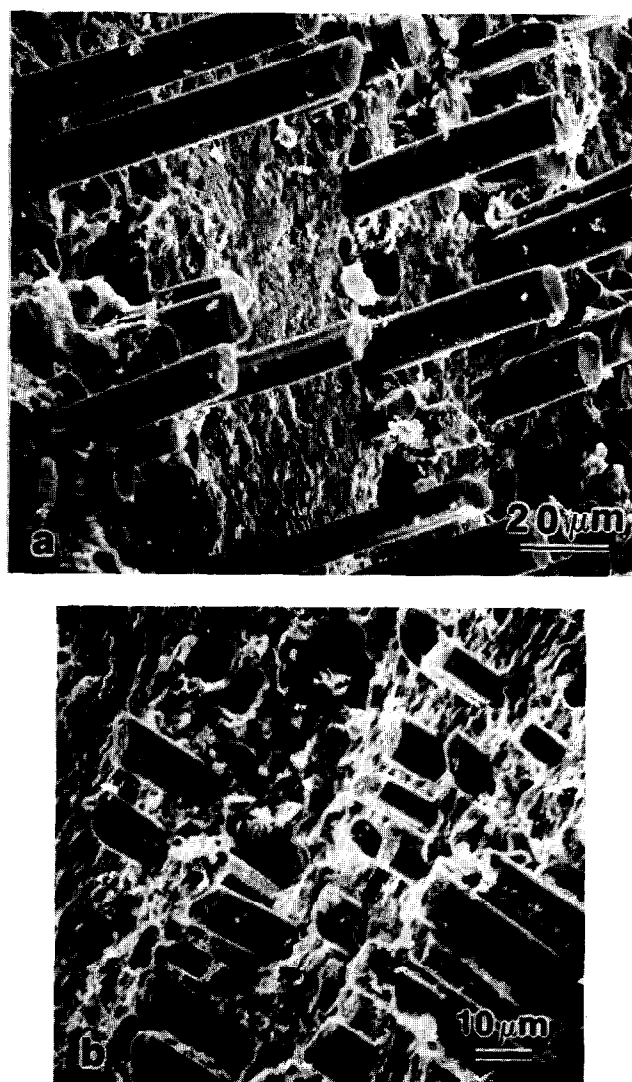


Fig. 9. Fracture surface of BN/SiC coated Nextel 550/mullite composites: (a) hot-pressed and (b) hot-pressed + heat-treated.

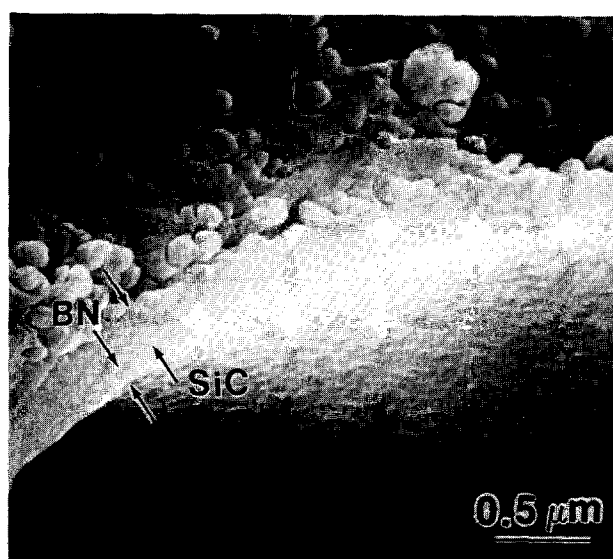


Fig. 10. Fracture surface of SiC/BN coated Nextel 550/mullite composite showing a hole formed in the matrix as a result of fiber pullout. Note the double coating left in the matrix during fiber pullout and the strong bonding between the matrix and the SiC coating.

References

1. Prewo, K. M. & Batt, J. A., The oxidative stability of carbon fibre reinforced glass-matrix composites. *J. Mater. Sci.*, **23** (1988) 523–7.
2. Mah, T., Hecht, N. L., McCullum, D. E., Hoenigman, J. R., Kim, H. M., Katz, A. P. & Lipsitt, H. A., Thermal stability of SiC fibres (Nicalon). *J. Mater. Sci.*, **19** (1984) 1191–201.
3. Hermes, E. E. & Kerans, R. J., Degradation of non-oxide reinforcement and oxide matrix composites. *Mat. Res. Soc. Symposium Proceedings*, **125** (1988) 73–8.
4. Singh, R. N. & Brun, M. K., Effect of boron nitride coating on fiber-matrix interactions. *Ceram. Eng. Sci. Proc.*, **8** (1987) 636–43.
5. Yeheskel, O., Balmer M. L. & Cranmer, D. C., Interfacial chemistry of mullite/mullite composites. *Ceram. Eng. Sci. Proc.*, **9** (1988) 687–94.
6. Michalske, T. A. & Hellmann, J. R., Strength and toughness of continuous-alumina-fiber-reinforced glass-matrix composites. *J. Am. Ceram. Soc.*, **71** (1988) 725–31.
7. Fitzer, E. & Schlichting, J., Fiber-reinforced refractory oxides. *High Temperature SiC*, **13** (1980) 149–72.
8. Lehman, R. L. & Doughan, C. A., Carbon coated alumina fiber/glass matrix composites. *Comp. Sci. & Tech.*, **37** (1990) 149–64.
9. Rice, R. W., BN coating of ceramic fibers for ceramic matrix composites. *US Patent*, **4**, 642,271, Feb. 10, 1987.
10. Ha, J.-S., Chawla, K. K. & Engdahl, R. E., Effect of processing and fiber coating on fiber-matrix interaction in mullite fiber–mullite matrix composites. *Mater. Sci. & Eng.*, **A161** (1993) 303–8.
11. Johnson, D. D., Hiltz, A. R. & Grether, M. F., Properties of Nextel 480 ceramic fibers. *Ceram. Eng. Sci. Proc.*, **8** (1987) 744–54.
12. Experimental Product Data Sheet, Ceramic Materials Department, 3M Co., St. Paul, Minnesota.
13. Ceramic Sources, Vol. 1, American Ceramic Society, 1985 pp. 336 and 350.
14. Skoog, A. & Moore, R., Refractory of the past for the future: mullite and its use as a bonding phase. *Am. Ceram. Soc. Bull.*, **67** (1988) 1180–5.
15. Kumazawa, T., Ohta, S., Kanzaki, S., Sakaguchi, S and Tabata, H., Elastic properties of mullite ceramics at elevated temperature. *J. Mater. Sci.*, **8** (1989) 47–8.
16. Blocher, Jr, J. M., Nitrides. In *High-Temperature Materials and Technology*, Chap. 11, eds I. E. Campbell & E. M. Sherwood, John Wiley & Sons, New York, 1967, p. 379.
17. Williams, D. S., Elastic stiffness and thermal expansion coefficient of boron nitride films. *J. Appl. Phys.*, **57** (1985) 2340–2.
18. Hampshire, S., Engineering properties of nitrides. In *Engineered Materials Handbook*, Vol. 4: Ceramics and Glasses, ed. S. J. Schneider, ASM International, 1991, p. 819.
19. Shaffer, P. T. B., Engineering properties of carbides. In *Engineered Materials Handbook*, Vol. 4: Ceramics and Glasses, ed. S. J. Schneider, ASM International, 1991, p. 808.
20. Sacks, M. D., Lee, H.-W. & Pask, J. A., A review of powder preparation methods and densification procedures for fabricating high density mullite. In *Ceramic Transactions*, Vol. 6: Mullite and Mullite Matrix Composites, Eds S. Somiya, R. F. Davis and J. A. Pask, American Ceramic Society, Westerville, OH, 1990, p. 167.
21. Aksay, A., Dabbs, D. M. & Sarikaya, M., Mullite for structural, electronic and optical applications. *J. Am. Ceram. Soc.*, **74** (1991) 2343–58.
22. Chawla, K. K., *Ceramic Matrix Composites*, Chapman & Hall, London, 1993, p. 128.
23. Ha, J.-S. & Chawla K. K., The effect of precursor characteristics on the crystallization and densification of diphasic mullite gels. *Ceramics International*, **19** (1993) 299–305.
24. Ha, J.-S. & Chawla, K. K., Effect of SiC/BN double coating on fibre pullout in mullite fibre/mullite matrix composites. *J. Mater. Sci. Lett.*, **12** (1993) 84–6.
25. Chawla, K. K., Xu, Z. R., Ha, J.-S., Lara-Curzio, E., Ferber, M. K. & Russ, S., Interfacial characteristics of mullite fiber/BN/coating/mullite matrix composites. In *Pro. Advanced Ceramic Matrix Composites*, ed. J. P. Singh, Amer. Ceram. Soc., 1994, p. 779.
26. Chawla, K. K., *Ceramic Matrix Composites*, Chapman & Hall, London, 1993, p. 325.
27. Lara-Curzio, E. & Ferber, M. K., *J. Mater. Sci.*, 1994, in press.
28. Hsueh, C.-H., Evaluation of interfacial properties of fiber-reinforced ceramic composites using a mechanical properties microprobe. *J. Am. Ceram. Soc.*, **76** (1993) 3041–50.
29. Kerans, R. J. & Parathasarathy, T. A., Theoretical analysis of the fiber pullout and pushout tests. *J. Am. Ceram. Soc.*, **74** (1991) 1585–96.